A

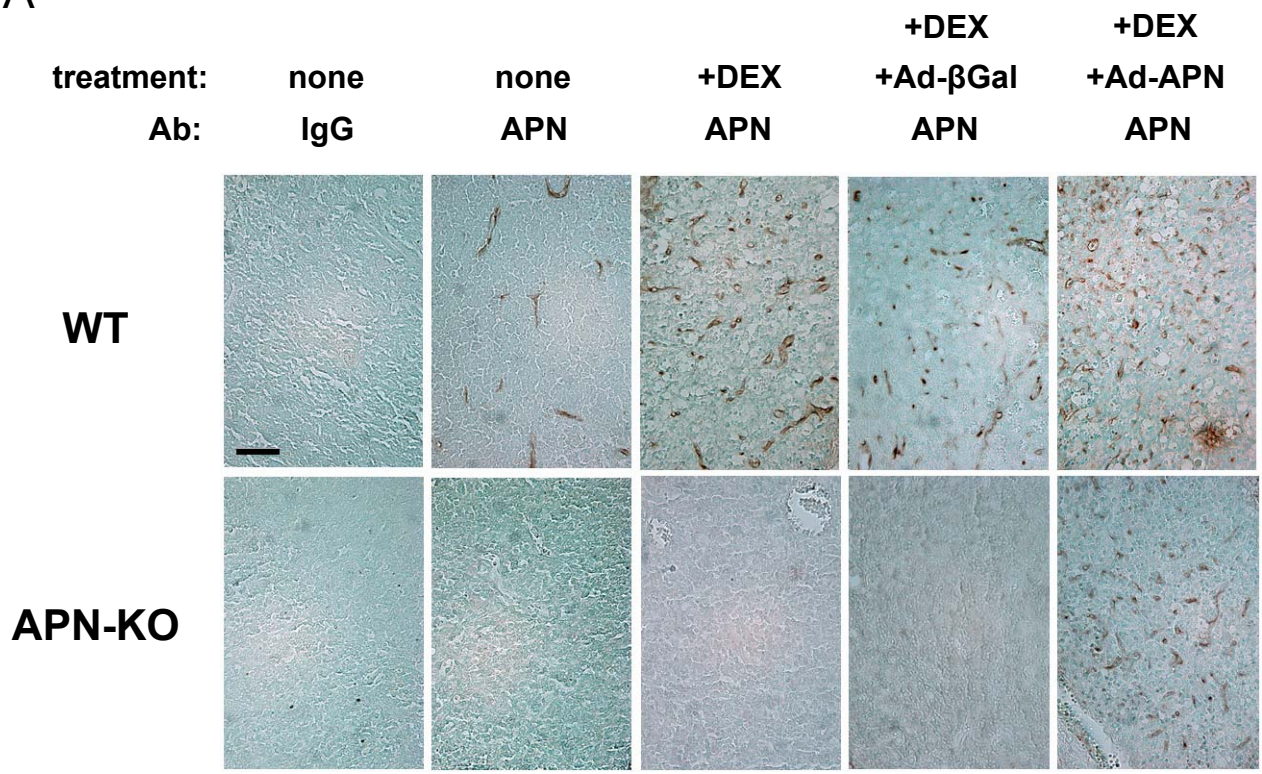

B

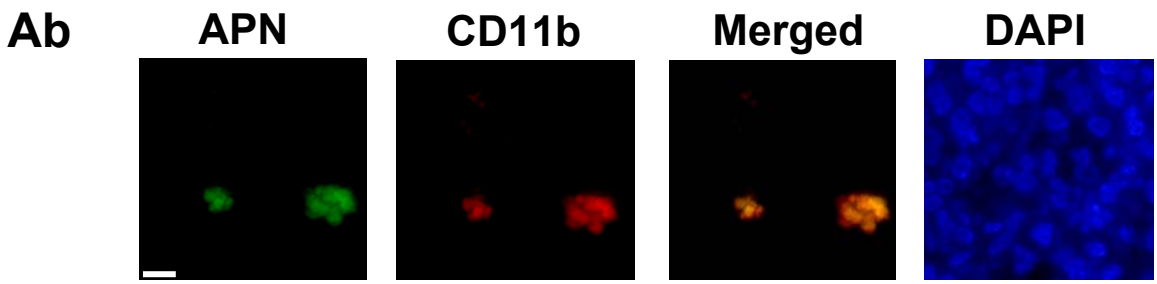

Supplemental Figure.1

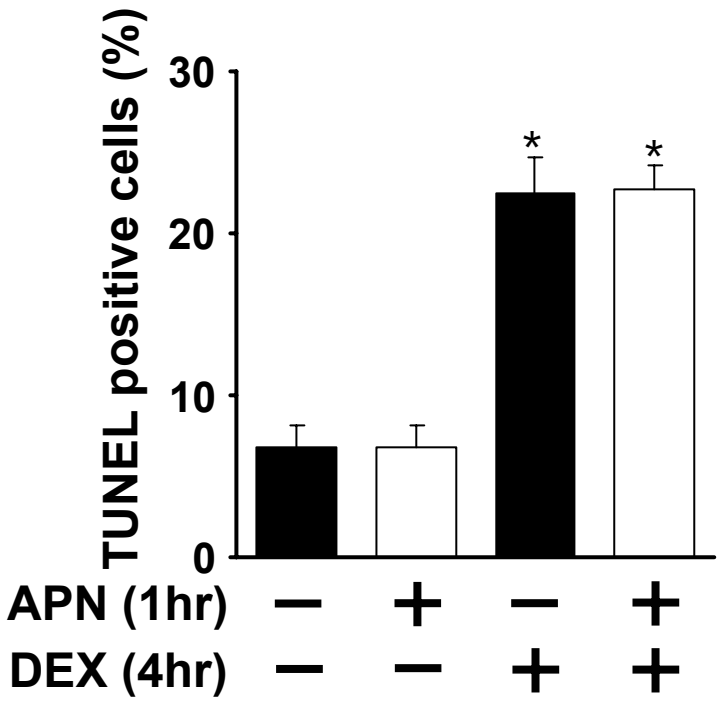

Supplemental Figure.2

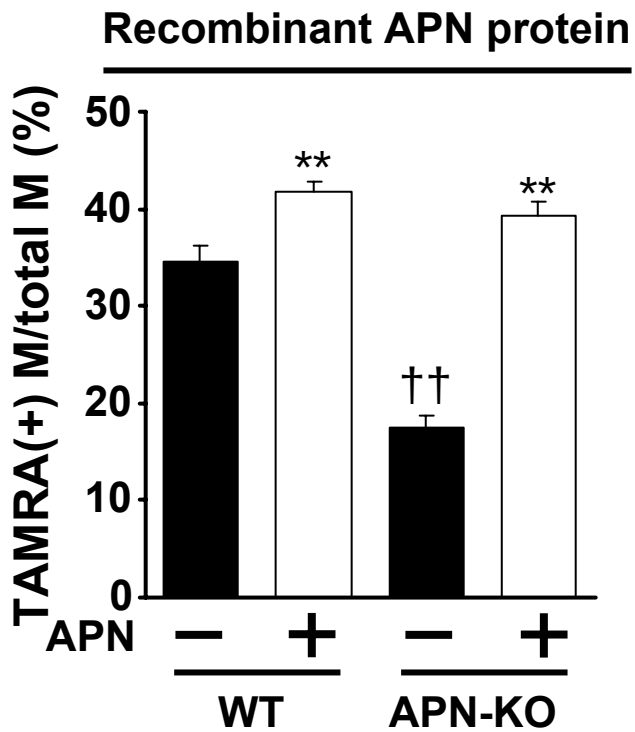

Supplemental Figure.3

A

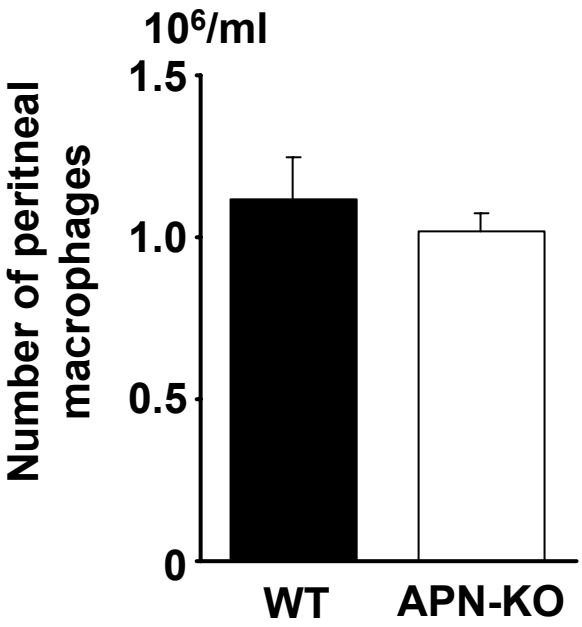

B

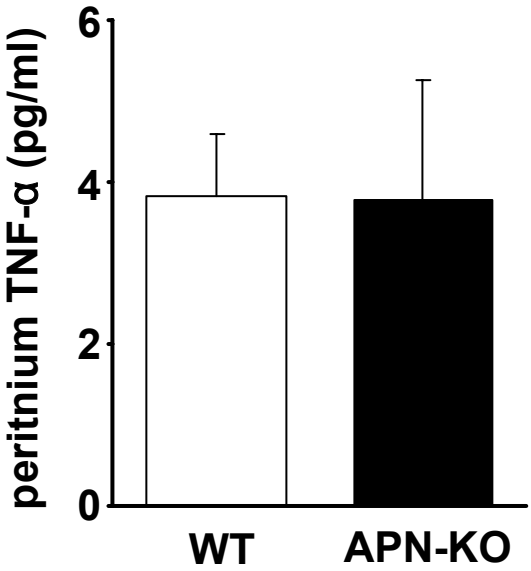

Supplemental Figure.4

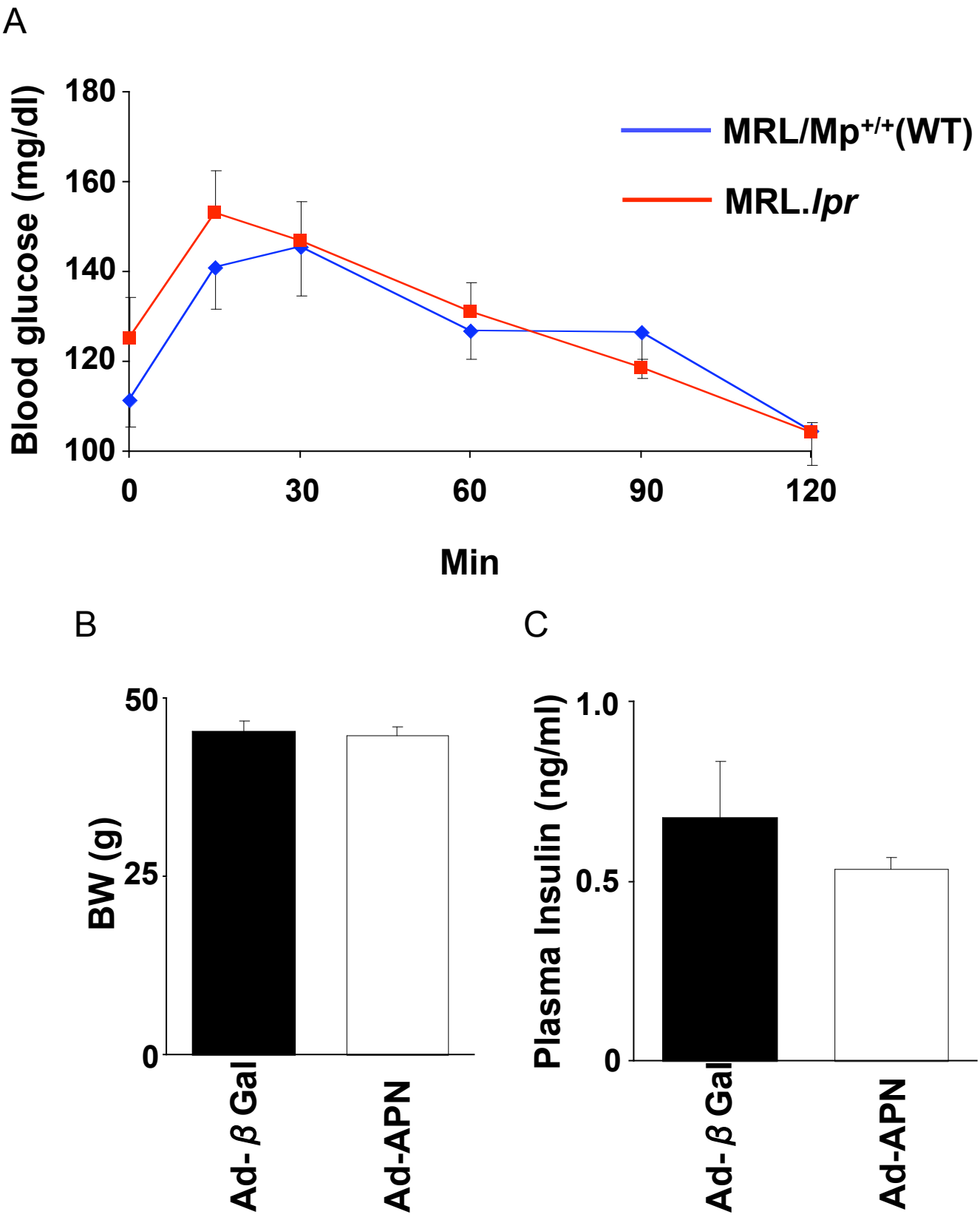

Supplemental Figure.5

D

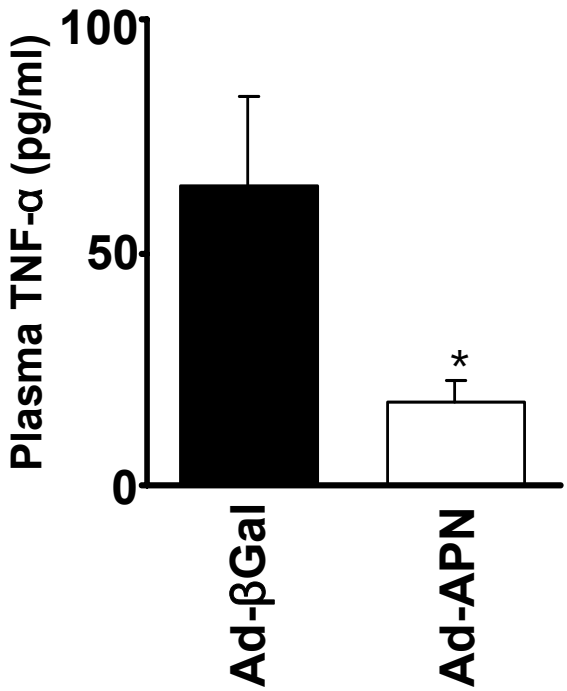

Supplemental Figure.5

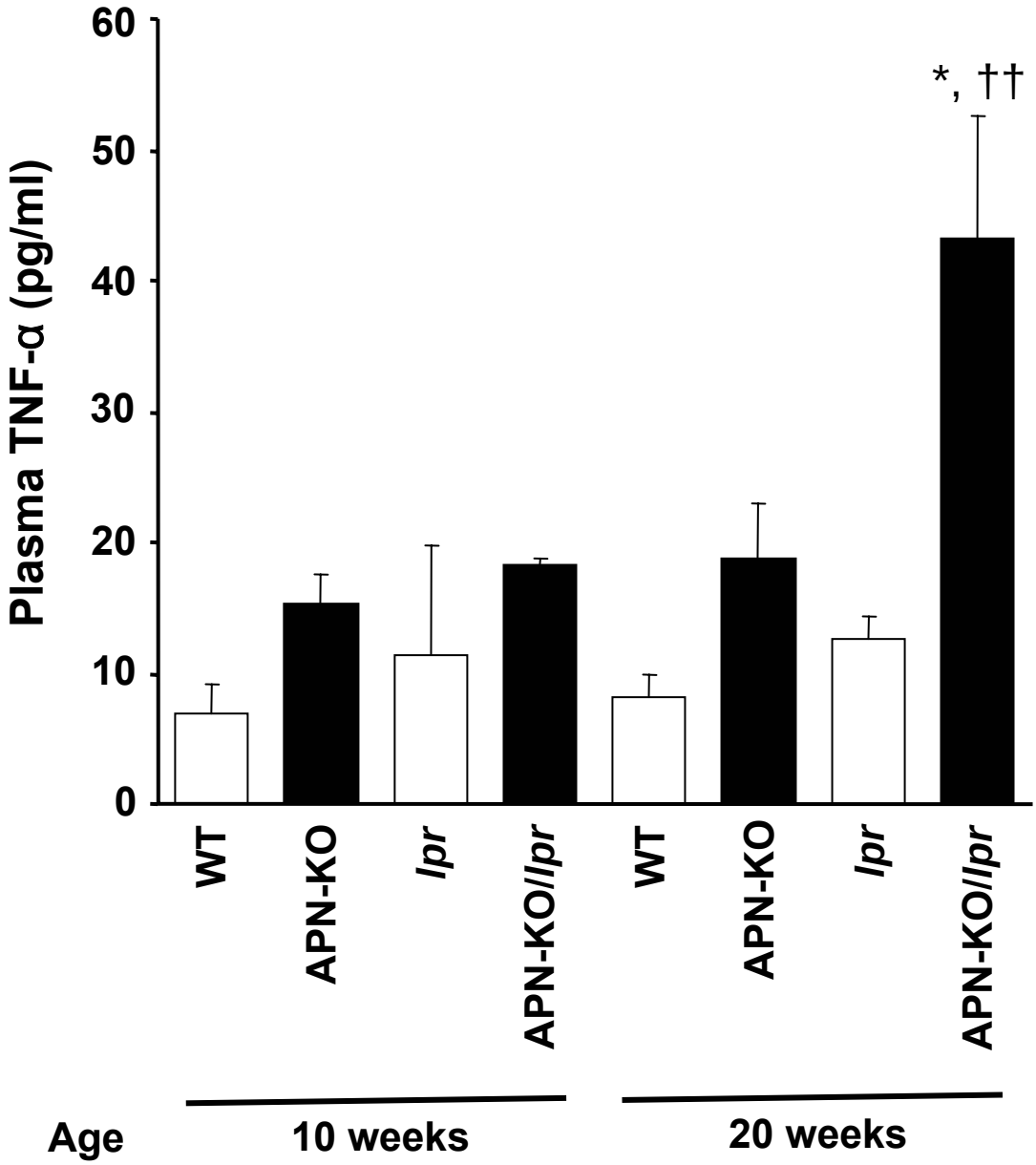

Supplemental Figure.6

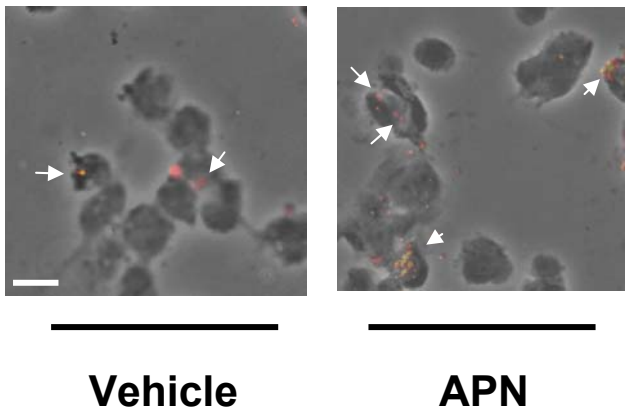

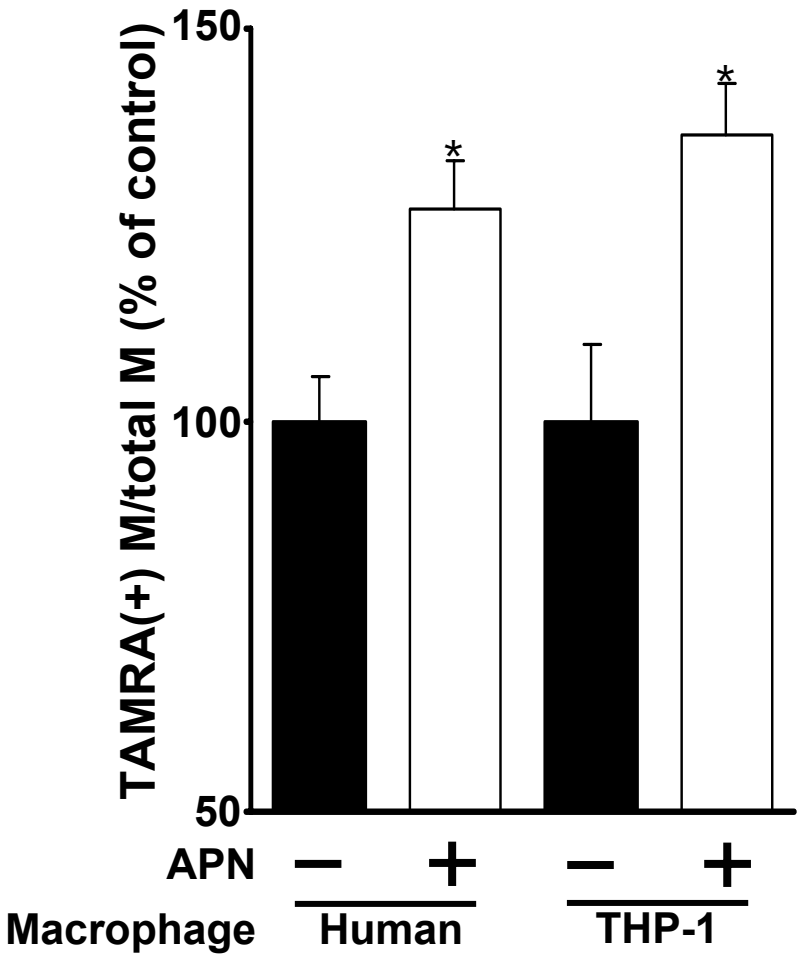

Supplemental Figure.7

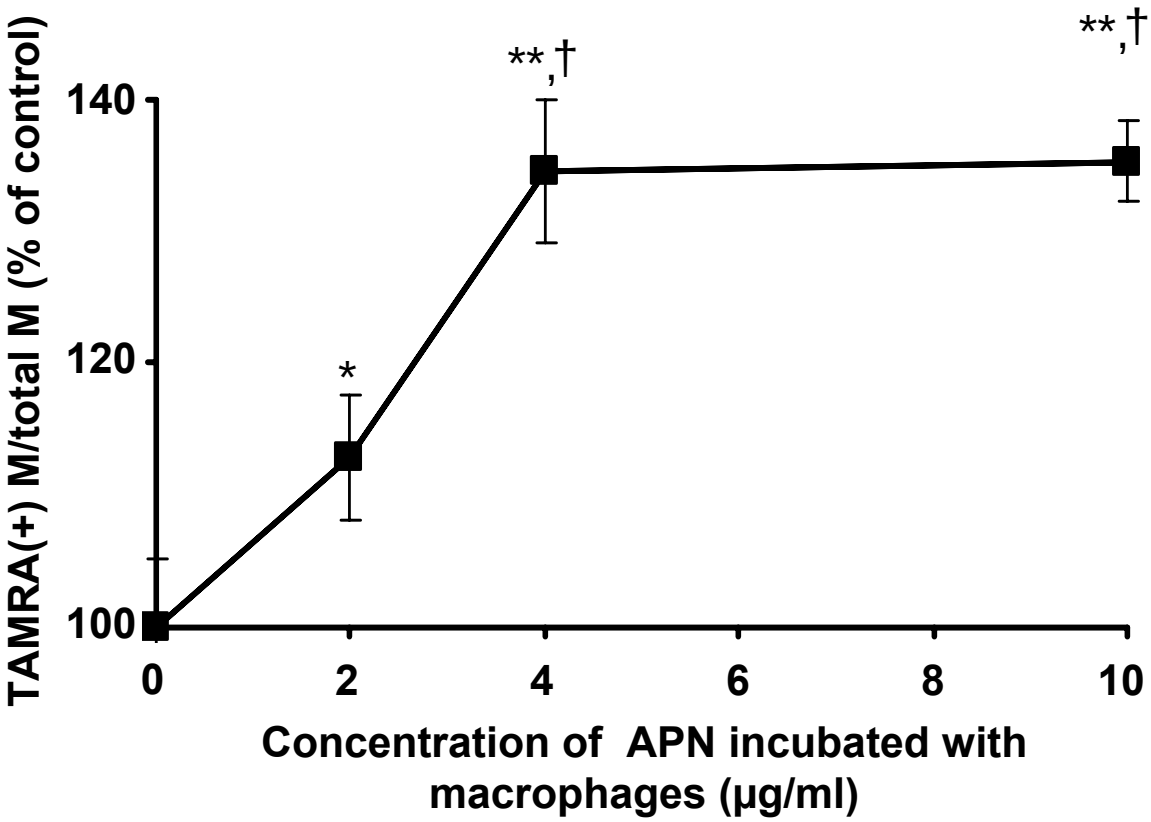

Supplemental Figure.8

A

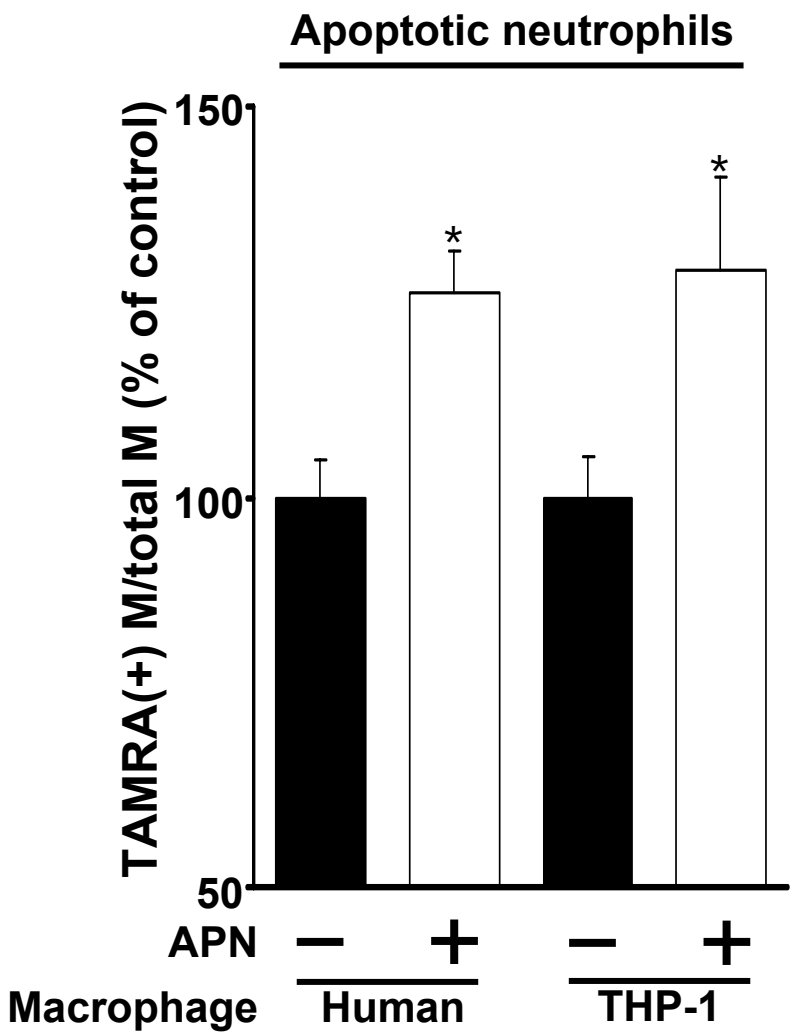

Supplemental Figure.9

B

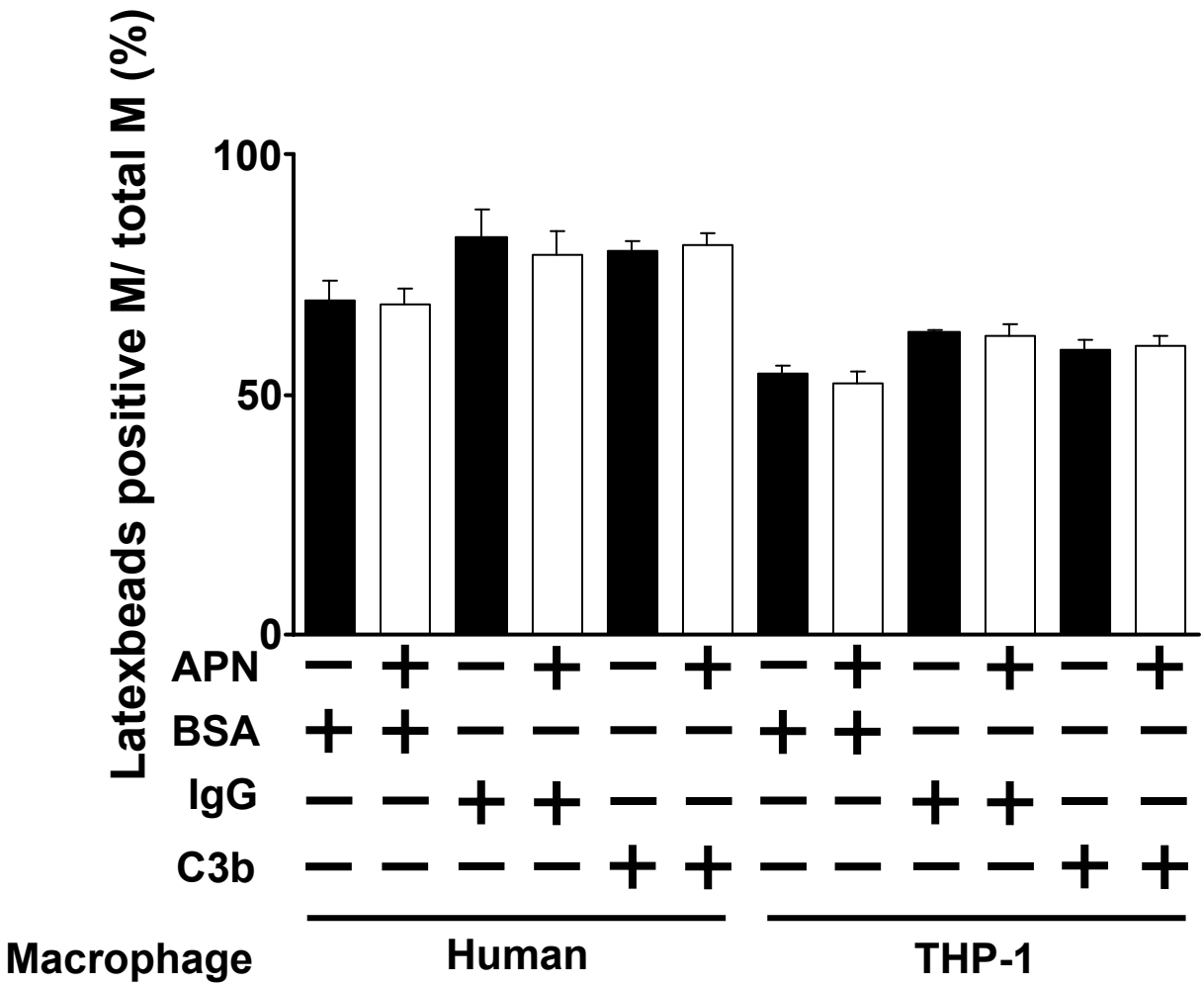

Supplemental Figure.9

C

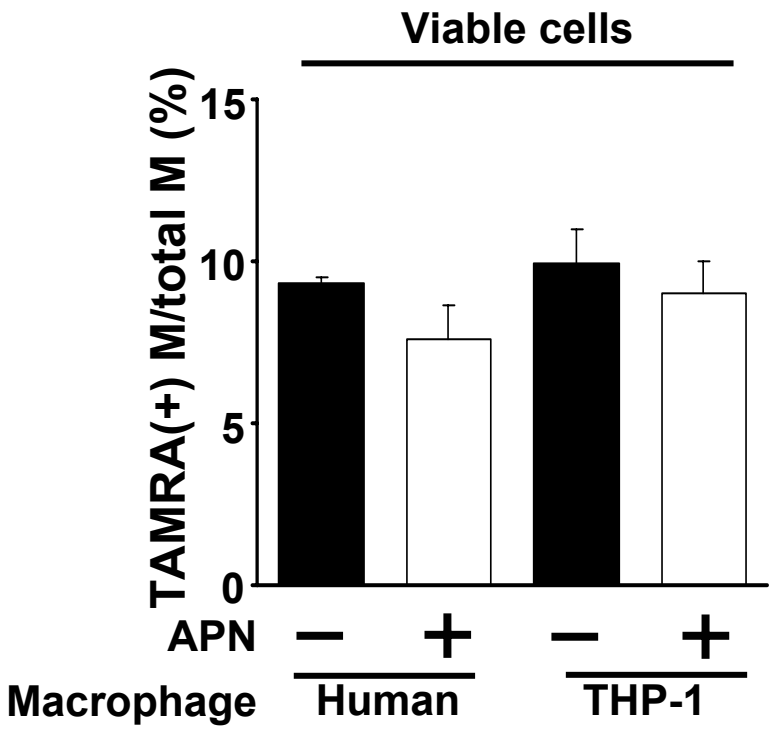

D

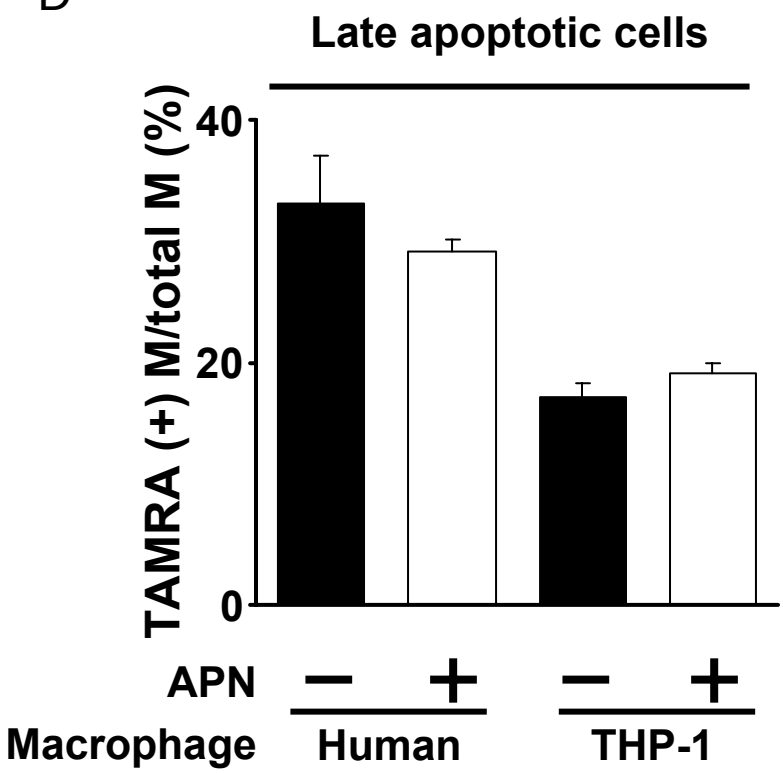

Supplemental Figure.9

A

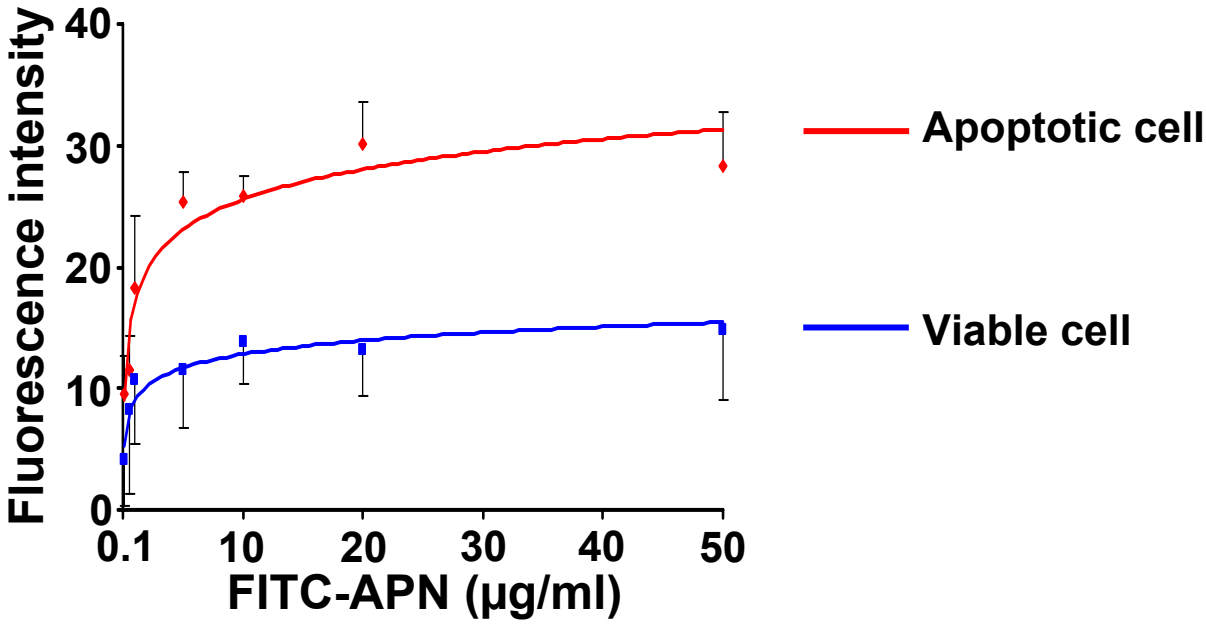

B

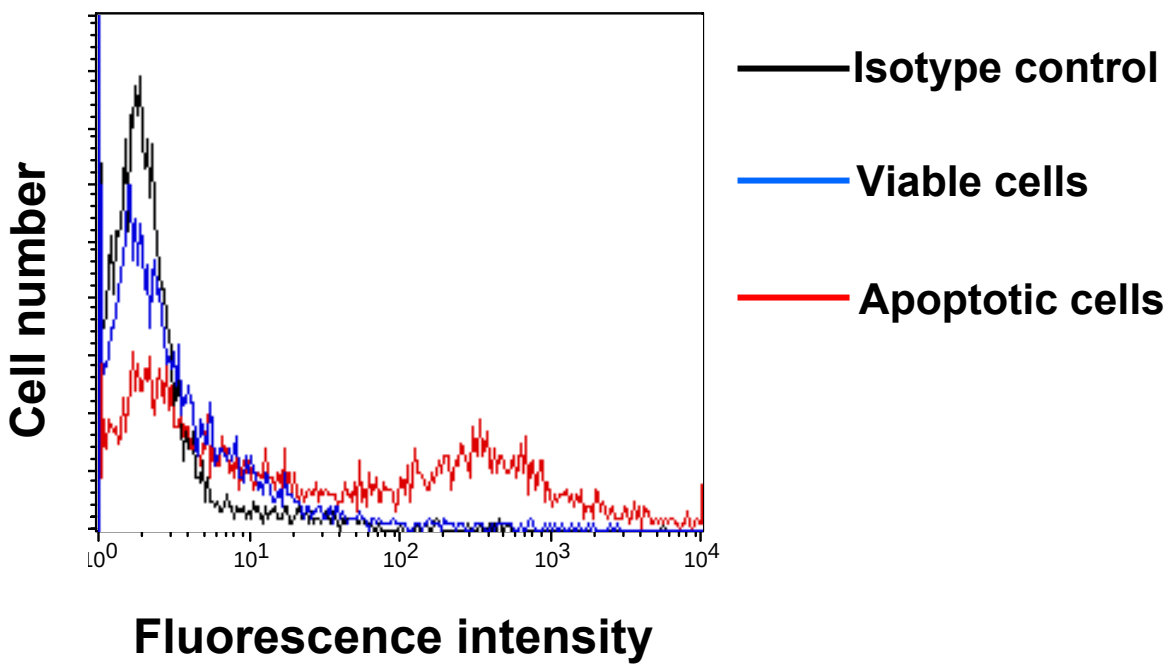

Supplemental Figure.10

C

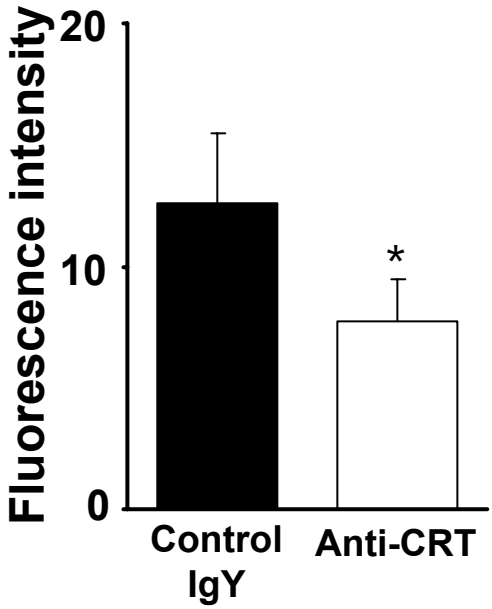

D

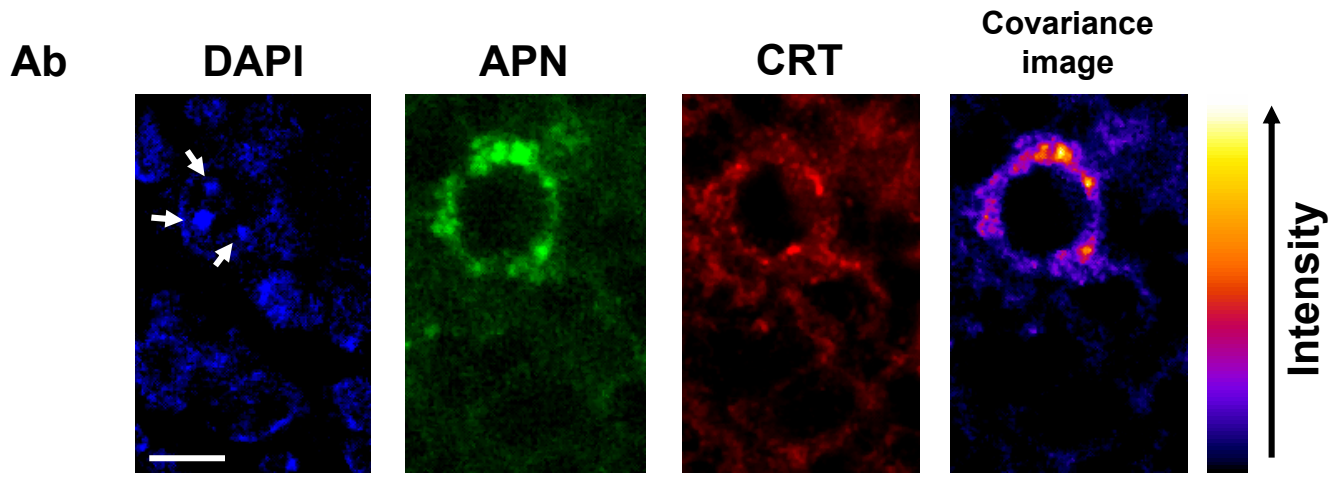

Supplemental Figure.10

A

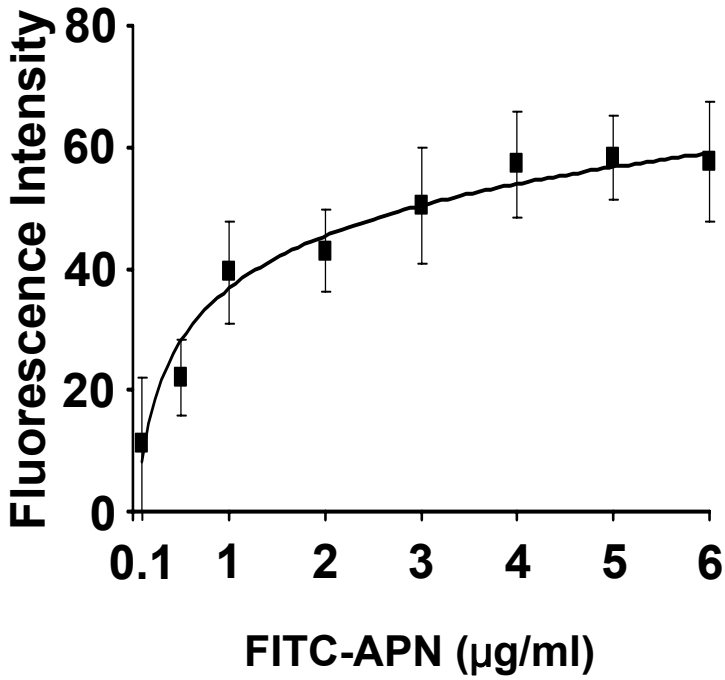

B

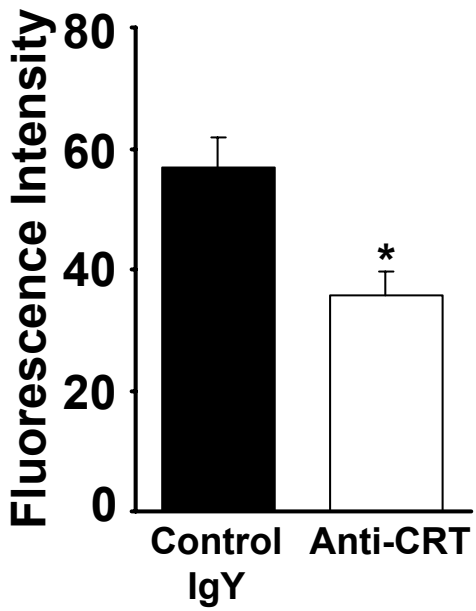

Supplemental Figure.11

C

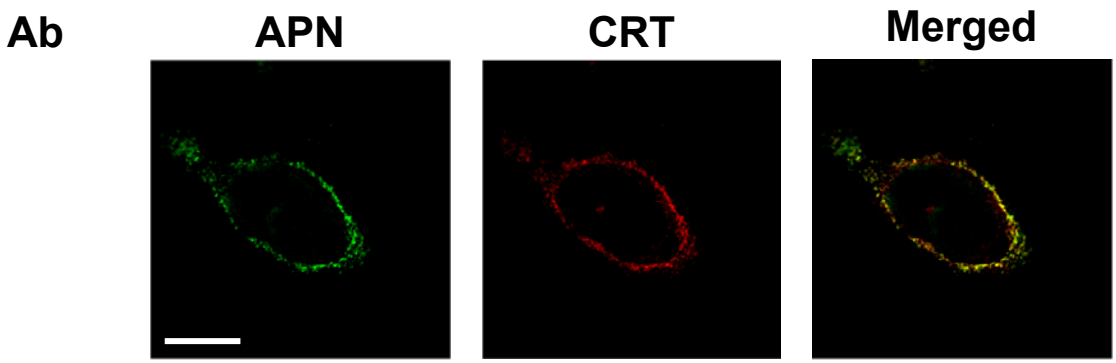

Supplemental Figure.11

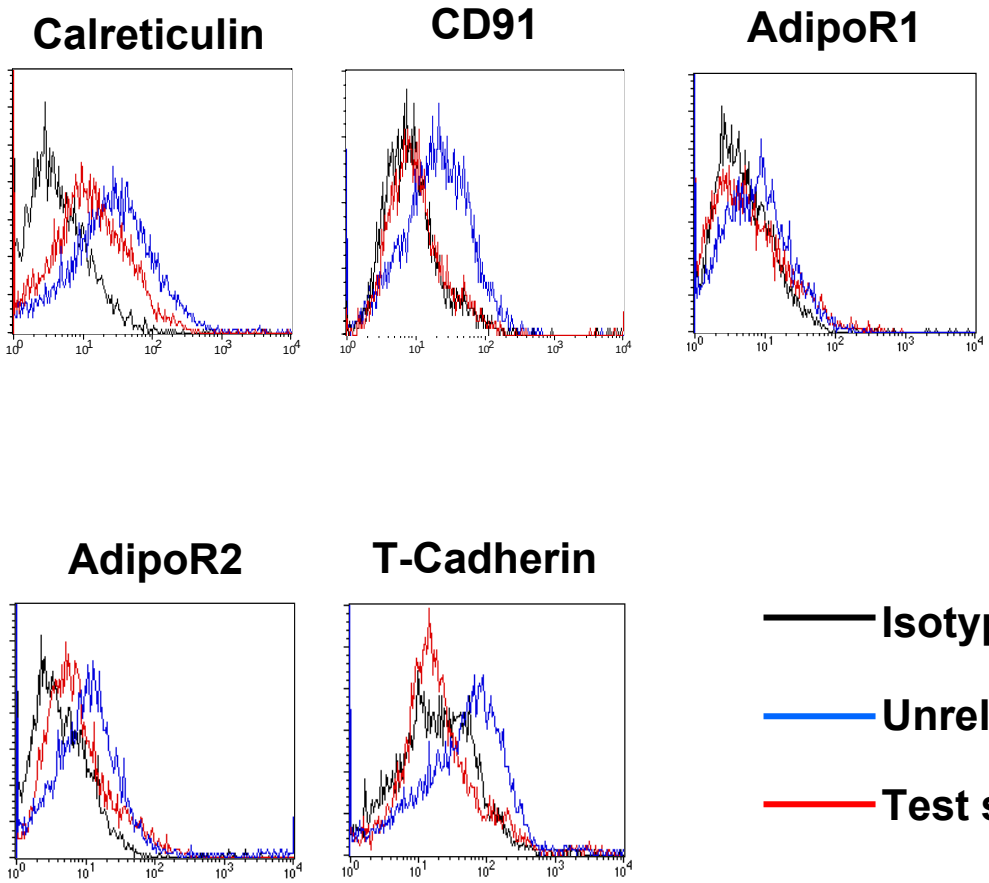

Supplemental Figure.12

Supplemental Figure Legends

Supplemental Figure 1. Adiponectin accumulates in damaged thymi and colocalizes with macrophages. (A) Immunohistochemical analysis of thymi of wild-type and APN-KO mice. The adiponectin signal increased in the thymus of wild-type mice following injury with dexamethasone. Control IgG consistently showed no evidence of staining. Thymi sections from APN-KO mice showed no staining with adiponectin antibody, except in the case of Ad-APN treated animals. Bar = 50 μm. **(B)** Adiponectin colocalized macrophages in mouse thymi. The thymi of wild-type mice treated with DEX followed by Ad-APN treatment were used. Sections were stained with anti-mouse adiponectin antibody (green) and anti-mouse CD11b antibody (red). Colocalization is indicated by yellow in the merged image. Bar = 10 μm.

Supplemental Figure 2. Recombinant adiponectin does not protect thymocytes from apoptosis induced by dexamethasone in vitro. Thymocytes were collected from wild type mice and were preincubated with human recombinant adiponectin (50 μg/ml) for 1 hr prior to stimulation of DEX (1 μM) or vehicle for 4 hr. TUNEL-positive (apoptotic) thymocytes were assessed by fluorescent microscopic analysis. * P <0.05 versus control (n = 3-6).

Supplemental Figure 3. Local administration of human recombinant adiponectin protein increases uptake of apoptotic cells by macrophages in vivo. TAMRA, SE-labeled early apoptotic Jurkat T cells were preincubated for 1 hr with baculovirus-produced APN (50 μg/ml) or vehicle prior to injection into the peritoneal cavity. After 30 min, macrophage phagocytosis was assessed by flow cytometry. Macrophages were stained with FITC-conjugated anti-F4/80 antibody and the percentage of phagocytic macrophages (M) was calculated as TAMRA, SE-positive (+) macrophages (M)/total M X 100%. ** P < 0.01 versus vehicle (n = 6).

Supplemental Figure 4. Peritoneal macrophages and TNF-α levels induced by thioglycollate injection are similar in APN-KO and WT mice. (A) Peritoneal macrophages were collected with 5 ml of lavage fluid 3 days after thioglycollate injection

into abdominal cavity. Collected macrophages were stained with Diff Quik are counted by microscopy. **(B)** TNF-α levels in lavage supernatant from abdominal cavity was determined by ELISA (n = 3-4).

Supplemental Figure 5. Systemic delivery of adiponectin reduces plasma TNF-α levels in MRL.*lpr* mice without influencing metabolic parameters. (A) MRL.*lpr* had normal glucose sensitivity at the age of 18 weeks. Glucose tolerance tests were performed on MRL/Mp$^{+/+}$ (WT) and MRL.*lpr* mice after 6 h fasting. After peritoneal injection of 1g/kg glucose, blood samples were collected and assayed for blood glucose. (*n* = 5-7). **(B)** Body weight (BW) was not different after 2 weeks in MRL.*lpr* administered Ad-βgal or Ad-APN (*n* = 8). **(C)** Circulating insulin levels were not different in MRL.*lpr* administered Ad-βgal or Ad-APN. Blood samples were collected after 6 h fasting (*n* = 3-4). **(D)** Administration of Ad-APN significantly reduced plasma TNF-α levels in MRL.*lpr* mice. TNF- α levels were measured 2 weeks after injection of Ad-APN or Ad-βgal. **P* < 0.05 versus Ad-βgal (*n* = 8).

Supplemental Figure 6. Adiponectin-deficient B6.*lpr* mice display increased plasma TNF-α levels. Blood samples of each type of mice were collected at the age of 10 weeks and 20 weeks. **P*<0.05 versus APN-KO; ††*P* < 0.01 versus WT and *lpr* (*n* = 4-13).

Supplemental Figure 7. Adiponectin promotes the phagocytosis of apoptotic cells by microscopic analysis. TAMRA, SE-labeled apoptotic Jurkat T cells were preincubated for 1 hr with baculovirus-produced adiponectin from (50 μg/ml) or vehicle. Human monocyte-derived macrophages or differentiated THP-1 cells were then incubated for 30 min with the labeled Jurkat cells under conditions where the concentration of APN was diluted to 10 μg/ml. Phagocytosis was assessed by microscopy, and representative pictures for 2 experimental conditions using THP-1 macrophages are shown. White arrows indicate ingested TAMRA, SE-positive apoptotic Jurkat T cells. Bar =20 μm. The percentage of phagocytic macrophages was calculated as TAMRA, SE-positive (+) macrophages (M)/total M X 100%. Control is 20.4 ± 1.1% (human) and 15.5 ± 1.5% (THP-1). **P* < 0.05 versus vehicle (*n* = 8).

Supplemental Figure 8. Adiponectin promotes the phagocytosis of apoptotic bodies in a dose-dependent and saturable manner. TAMRA, SE-labeled apoptotic Jurkat T cells were preincubated for 1 hr with baculovirus-produced adiponectin (10, 20 or 50 μg/ml) or vehicle. Human monocyte-derived macrophages were then incubated for 30 min with TAMRA, SE-labeled Jurkat T cells, under conditions where the concentration of APN was diluted to 2, 4 or 10 μg/ml. Phagocytosis was assessed by flow cytometry. Macrophages were stained with FITC-conjugated anti-human macrophage antibody and the percentage of phagocytic macrophages was calculated as TAMRA, SE-positive (+) macrophages (M)/total M X 100%. The percentage of phagocytic macrophages in the absence of adiponectin is 34.3 ± 1.8%. $*P < 0.05$, $**P < 0.01$ versus vehicle, $\dagger P < 0.05$ versus 2 μg/ml (n = 9-10).

Supplemental Figure 9. **Adiponectin promotes the phagocytosis of apoptotic neutrophils but not IgG-, C3b-opsonized microbeads, viable cells or late apoptotic cells. (A)** Recombinant adiponectin increases uptake of apoptotic human neutrophils. TAMRA, SE-labeled apoptotic neutrophils are preincubated for 1 hr with baculovirus-produced adiponectin (50 μg/ml) or vehicle. Human monocyte-derived macrophages and THP-1 cells were then incubated for 30 min with TAMRA, SE-labeled neutrophils under conditions where adiponectin was diluted to 10 μg/ml. Phagocytosis was assessed by microscopy. The percentage of phagocytic macrophages was calculated as TAMRA, SE-positive (+) macrophages (M)/total M X 100%. Phagocytic macrophage of control is 21.1 ± 0.9% (human) and 18.5 ± 1.0% (THP-1) $*P < 0.05$ versus vehicle (n = 8). **(B)** Recombinant adiponectin did not increase the uptake of opsonized latex microbeads. 1.0 μm red fluorescent (580/605) FluoSpheres® carboxylate-modified microspheres (Invitrogen) were opsonized with BSA, human IgG or human C3b. Each opsonized fluorescent microbeads (1×10^7 beads) were treated with baculovirus-produced adiponectin and exposed to macrophages as described above. Phagocytosis was assessed by flow cytometry as described above (n = 4). **(C)** Recombinant adiponectin did not increase the uptake of viable Jurkat T cells. TAMRA, SE-labeled viable Jurkat T cells were preincubated for 1 hr with recombinant adiponectin or vehicle, and exposed to human monocyte-derived macrophages or THP-1 cells as described above. Phagocytosis

was assessed by flow cytometry (n = 4). **(D)** Recombinant adiponectin did not increase the uptake of late apoptotic Jurkat T cells. TAMRA, SE-labeled late apoptotic Jurkat T cells were preincubated for 1 hr with recombinant adiponectin or vehicle and exposed to human monocyte-derived macrophages or THP-1 cells as described above. Late apoptotic cells stained positive with propidium iodide, but early apoptotic cells did not. Phagocytosis was assessed by flow cytometry (n = 3-6).

Supplemental Figure 10. **Adiponectin binding to viable and apoptotic cells. (A)** Saturable binding of recombinant adiponectin to early apoptotic and viable Jurkat T cells. Apoptotic and viable Jurkat T cells were incubated with increasing concentrations of FITC-conjugated adiponectin and binding was assessed with a fluorescent microplate reader. The data were analyzed with Microsoft Excel to produce a logarithmic trend line. (B) The expression of calreticulin is increased on the surface of apoptotic Jurkat T cells. Early apoptotic and viable Jurkat T cells were stained with anti-calreticulin antibody or isotype control followed by treatment with FITC-conjugated secondary antibody. The expression of cell surface calreticulin was analyzed by flow cytometry. Representative data are shown. **(C)** Anti-calreticulin antibody inhibits the binding of adiponectin to apoptotic Jurkat T cells. Early apoptotic and viable Jurkat T cells were incubated with 10 μg FITC-APN for 60 min in the presence of anti-calreticulin antibody (200 μg/ml) or control chicken IgY (200 μg/ml) for 60 min. Fluorescence intensity was measured with a microplate reader and corrected by substrating the fluorescence intensity of viable cells. *P < 0.05 versus control IgY (n=8)**. (D)** Adiponectin colocalizes with calreticulin on apoptotic thymocytes using two-photon confocal microscopy. Thymus sections were stained with anti-mouse adiponectin antibody (green), anti-calreticulin antibody (red) and DAPI (blue). White arrows show nuclear fragmentation in the apoptotic cell. The covariance image shows the relative degree of colocalization at each pixel. Bar = 5 μm.

Supplemental Figure 11. Adiponectin interacts with calreticulin on the macrophage cell surface. (A) Saturable binding of recombinant adiponectin to intact macrophages. THP-1 macrophages were incubated with increasing concentrations of FITC-conjugated

adiponectin, and binding was assessed with a fluorescent microplate reader. The data were analyzed with Microsoft Excel to produce a logarithmic trend line. **(B)** Anti-calreticulin antibody inhibits the binding of adiponectin to THP-1 macrophages. THP-1 macrophages were incubated with 6 μg FITC-APN for 60 min in the presence of anti-calreticulin antibody (200 μg/ml) or control chicken IgY (200 μg/ml) for 60 min. Fluorescence intensity was measured with a microplate reader $*P < 0.05$ ($n = 8$). **(C)** Adiponectin and calreticulin are colocalized on the surface of macrophages. THP-1 macrophages were incubated with human recombinant adiponectin (5 μg/ml) for 60 min. After washing, THP-1 cells were stained with anti-human adiponectin antibody followed by Alexa Fluor® 488 conjugated anti-goat IgG antibody. Cells were then stained with anti-calreticulin antibody followed by Alexa Fluor® 594 conjugated anti-rabbit IgG antibody. The double labeled THP-1 cells were analyzed by confocal microscopy. Representative images are shown. Adiponectin is shown in green, calreticulin in red, and adiponectin colocalization with calreticulin is indicated by yellow. Bar = 10 μm.

Supplemental Figure 12. Adiponectin receptor downregulation by siRNA. 1×10^6 differentiated THP-1 macrophages were transfected for 24 hr with 200 nM siRNA using Lipofectamine 2000 reagent. Controls were transfected with unrelated siRNA. The reduction in cell surface proteins was measured using a flow cytometer 72 hr after transfection. Representative data are shown.